Audio Engineering Society

Convention Paper

Presented at the 121st Convention
2006 October 5–8 San Francisco, CA, USA

An Extended Small Signal Parameter Loudspeaker Model for the Linear Array Transducer

Andrew D. Unruh[1], Richard W. Little[1], Christopher J. Struck[1], Ali Jabbari[1] , and Jens-Peter Axelsson[1]

[1] Tymphany Corporation, Cupertino, CA 95014 – USA
andy.unruh@tymphany.com , richard.little@tymphany.com , christopher.struck@tymphany.com , ali.jabbari@tymphany.com , jens-peter.axelsson@tymphany.com

ABSTRACT

The Linear Array Transducer (LAT) is a tubular form-factor loudspeaker driver technology which, to a good first approximation, can be modeled by the standard linear time invariant small signal parameter (SSP) loudspeaker circuit model. However, to understand the behavior of a LAT to a greater level of detail, the SSP model can be extended with the addition of eight additional mechanical parameters. In this paper the nature of these additional parameters in the model are explained. Further, an extended blocked impedance model is introduced that may be used with LATs or conventional loudspeakers. Additionally, the model is correlated to measurements of currently available LATs. Finally, it is shown how the LAT extended SSP model is approximated by the standard loudspeaker SSP model.

1. INTRODUCTION

1.1. Description of the Linear Array Transducer (LAT)

The LAT is an electro-dynamic loudspeaker typically employing a tubular form factor and two motors driving multiple opposing diaphragms. The motors are wired so that their voice coils move toward each other with positive voltages and away from each other with negative voltages. The motor on the left drives half of the diaphragms which are interleaved with those driven by the other motor. Thus adjacent diaphragms move in opposition to each other to generate sound. The arrangement of the moving masses leads to a design that results in a chassis that is nearly free of mechanically-induced vibration [1, 2]. The design is shown in Figure 1. Unlike conventional loudspeaker drivers, radiation is not direct. Therefore, we will introduce additional acoustical model elements to describe this behavior.

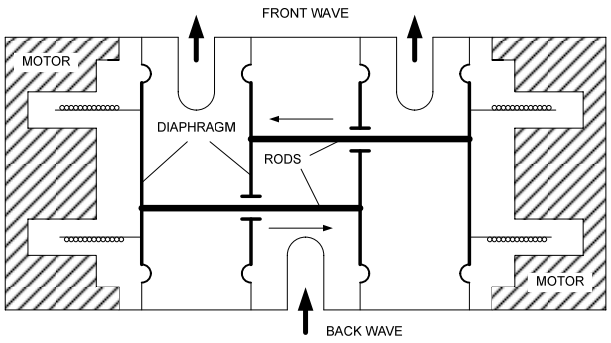

Fig. 1 Simplified diagram of the Linear Array Transducer (LAT), showing motors, front and rear ports, and direction of air flow for indicated diaphragm motion for three modular sections.

1.2. Objectives

The work described in this paper was performed with the goal of creating a linear, low frequency lumped parameter model of the LAT. In addition, the model is presented in a way that should be familiar to electroacoustic engineers. It should be usable by loudspeaker system designers using traditional software, and, of course, it should accurately describe the behavior of the LAT.

2. OBSERVED LAT BEHAVIOR

2.1. Electrical Impedance

Figure 2 shows the measured electrical impedance of a LAT having six diaphragms whose effective radiating area totals 525 cm^2. The impedance curve matches that of typical loudspeaker behavior, starting low near DC, increasing to a maximum near resonance, dropping down nearly to its DC value at a frequency labeled f_{MIN}, and then increasing again at high frequencies. As is typical of loudspeakers, the increase in impedance at very high frequencies is close to 3dB/octave rather than 6 dB/octave as would be expected if the high frequency impedance were dominated by a purely inductive load. This behavior is described as "semi-inductance" [3]. Another observed consequence of this behavior is that the impedance at f_{MIN} is somewhat higher than would be expected without the semi-inductance. It should be emphasized that the effects of semi-inductance are typical of electrodynamic loudspeakers and not specific to the LAT.

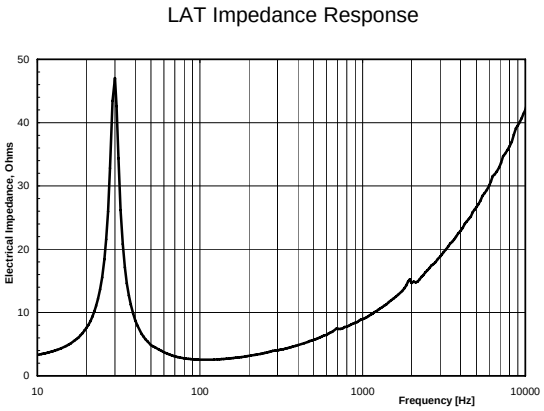

Fig. 2 Measured electrical impedance of a LAT

2.2. Frequency Response

Figure 3 shows the measured frequency response of the same LAT whose impedance response is shown in Figure 2. The infinite baffle frequency response was created by splicing a near field measurement (used at low frequencies) to a gated 2π measurement (used at high frequencies) with the LAT mounted into a standard baffle and box configuration [4]. The frequency response shown might be considered typical of a standard 12 inch woofer, although it does display a rather steep roll off in response above 1000 Hz.

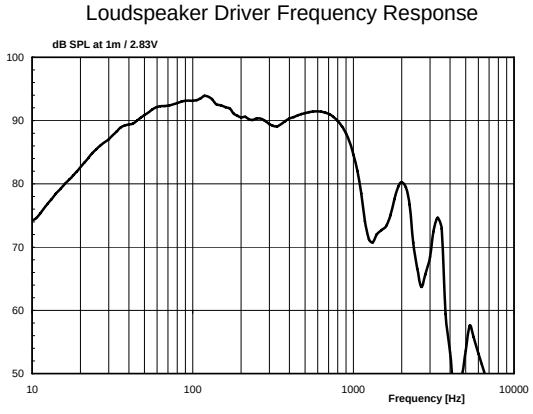

Fig. 3 Measured frequency response of a LAT

2.3. Air Leakage

The LATs used in this study incorporate holes in the diaphragms through which the drive rods pass. Alternating diaphragms are attached to a drive rod [1, 2]. Although the tolerances in the LAT are held very tight, there is still a small air gap, and therefore there is some amount of leakage between the front and rear chambers. The amount of leakage is dependent upon the design of the LAT and of the enclosure and typically results in a slight decrease in the device's output at low frequencies.

2.4. Effective Air Mass

A subset of the measured small signal parameters, as measured in free air, for a LAT incorporating six diaphragms with a total of 820 cm^2 of effective radiating area is shown in Table 1. Also shown in the table are the small signal parameters measured for the same LAT placed in a vacuum chamber. The difference between the two moving mass calculations must therefore be the effective mass due to air of the LAT. Using the standard formula [5] for calculating the effective mass due to air for a conventional driver with the same effective radiating area results in a mass of only 13g. Table 2 shows the same data for a LAT with an effective diaphragm area of 525 cm^2. In a conventional transducer with same effective radiating area, we would only expect to see about 7 grams of air mass.

	In Vacuum	**In Free Air**
Bl	16.62 T·m	16.74 T·m
M_{MS}	408 g	474 g
R_{MS}	17.11 kg/sec	17.22 kg/sec
C_{MS}	0.0563 mm/N	0.0610 mm/N

Table 1. A subset of the small signal parameters in vacuum and free air for a LAT with $S_D = 820cm^2$.

	In Vacuum	**In Free Air**
Bl	13.28 T·m	13.23 T·m
M_{MS}	174 g	200 g
R_{MS}	3.93 kg/sec	4.15 kg/sec
C_{MS}	0.159 mm/N	0.164 mm/N

Table 2. A subset of the small signal parameters in vacuum and in free air for a LAT with $S_D = 525cm^2$.

3. PROPOSED MODEL

3.1. Electrical Model

Previous work by Vanderkooy [3] showed that the blocked impedance of electrodynamic drivers is often dominated by a $\sqrt{j\omega}$ component. The elements showing the blocked impedance of the LAT is represented in the sub-circuit shown in Figure 4.

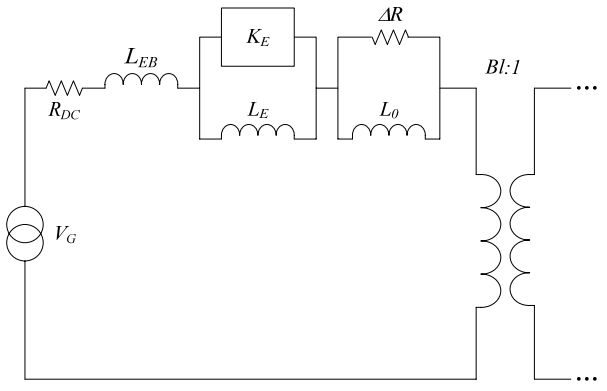

Fig. 4 Electrical equivalent sub-circuit model for the LAT.

The definitions of the terms in this sub-circuit are:

V_G applied open circuit voltage

R_{DC} DC resistance of the voice coil

Bl motor force constant

L_{EB} inductance of the part of the voice coil outside the motor gap

K_E "semi-inductance" term related to eddy current and skin depth behavior in the motor, with the impedance of this element represented mathematically by $K_E\sqrt{j\omega}$ [3, 6]

L_E inductance of the part of the voice coil located inside the motor gap

L_0 inductance representing the coupling of the coil to the motor [6]

ΔR eddy current losses in the motor [6]

Together, L_0 and ΔR represent that part of the low frequency behavior of the motor, in which the voice coil couples to the motor as if the motor were a single-turn resistive coil, and in which the skin depth is large. The K_E term, on the other hand, represents the higher frequency behavior of the motor, in which the skin depth is small.

However, the details of this blocked impedance model are beyond the scope of this paper. This may be addressed in a future paper. Here, we focus primarily on LAT-specific aspects of the model.

The total electrical impedance is

$$Z_{E,Total} = Z_{E,Blocked} + (Bl)^2 z_m \qquad (2)$$

where z_m is the mechanical mobility of the transducer, representing all of the circuit load to the right of the transformer shown in Figure 4.

3.2. Mechanical Model

The mechanical impedance model of the LAT is identical to that of conventional electrodynamic drivers. M_{MD} represents the combined mass of the diaphragms, voice coils, rods, and some portion of the suspension. C_{MS} represents the combined compliance of the suspension elements. R_{MS} represents the total mechanical viscous losses. S_D represents the total radiating area of the diaphragms.

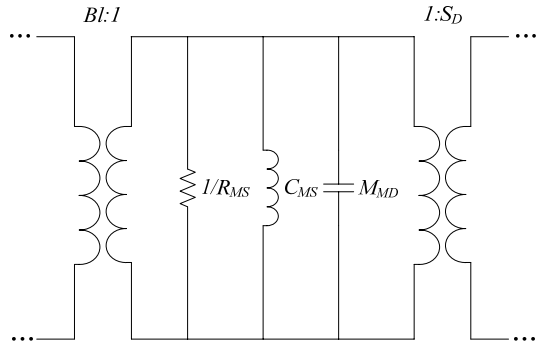

Fig. 5 Mechanical equivalent sub-circuit model for the LAT.

The equivalent sub-circuit representing the mechanical mobility of the LAT is shown in Figure 5.

The mechanical impedance is

$$Z_{MD} = s \cdot M_{MD} + R_{MS} + 1/(s \cdot C_{MS}) \qquad (3)$$

The mechanical mobility is

$$z_{MD} = \frac{1}{Z_{MD}} \qquad (4)$$

3.3. Acoustic Model

Figures 6 and 7 show a schematic representation of a LAT and a simplified version of the LAT used for model development with the analogous elements labeled. Note that while the electrical and mechanical models of the LAT are completely isomorphic with a conventional loudspeaker, it is necessary for the acoustic model to incorporate several extra elements. The front and rear cavities of the LAT represent the volumes of air between the diaphragms' front and rear surfaces, respectively. The respective front and rear ports represent the front and rear facing orifices of the LAT while the mesh hole in the diaphragm represents the leakage path in the LAT. Acoustically, the LAT can be represented by a transducer where the front and back of the diaphragm is connected by a small leak through the diaphragm and the diaphragms radiate into Helmholtz resonators.

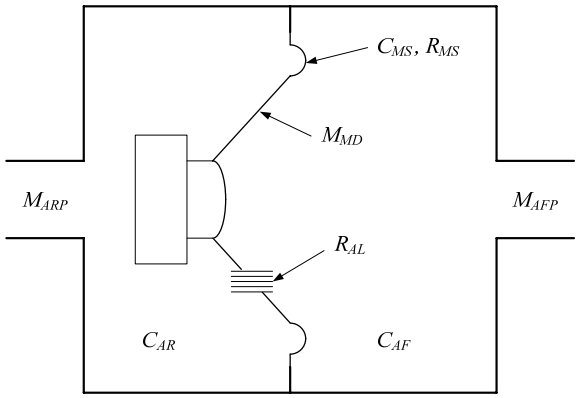

Fig. 6 Schematic representation of the mechanical and acoustical parameters of the LAT.

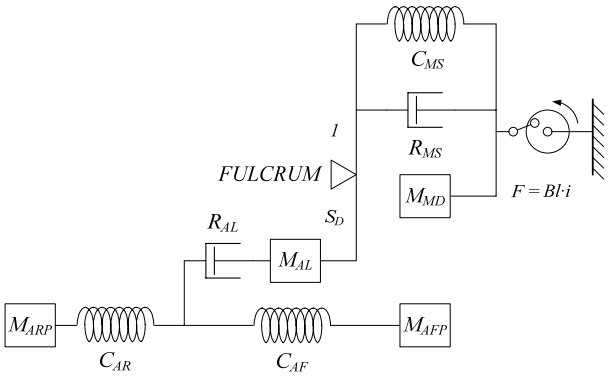

Fig. 7 Mobility model of the mechanical and acoustical parameters of the LAT.

Figure 7 shows the mechanical and acoustical free body diagram of the LAT. Figure 8 is the acoustical equivalent circuit, derived from Figure 7, of the LAT.

The acoustic impedance, neglecting the impedance to the room, can be calculated by inspection from Figure 8.

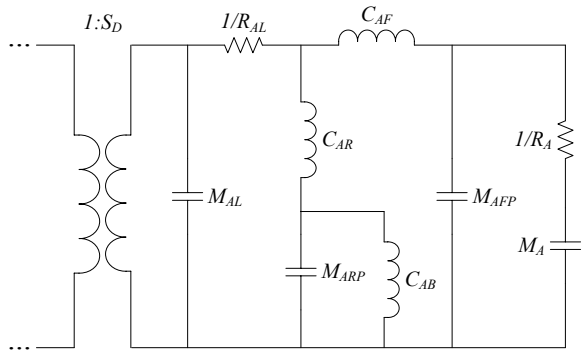

Fig. 8 Acoustical equivalent sub-circuit model for the LAT.

$$Z_A = \frac{R_{AL}\left(\frac{s \cdot M_{AFP}}{s^2 \cdot C_{AF} M_{AFP} + 1} + \frac{s \cdot M_{ARP}}{s^2 \cdot C_{AB} M_{ARP} + 1}\right)}{\left(R_{AL} + \frac{s \cdot M_{AFP}}{s^2 \cdot C_{AF} M_{AFP} + 1} + \frac{s \cdot M_{ARP}}{s^2 \cdot C_{AF} M_{ARP} + 1}\right)} \quad (7)$$

The definitions of terms in this relation and in Figure 8 are:

s	complex frequency variable
Z_A	acoustic impedance
R_{AL}	acoustic leak resistance
r_{AL}	acoustic leak responsiveness ($r_{AL} = 1/R_{AL}$)
M_{AL}	acoustic mass of the air in the leak
M_{AFP}	acoustic mass of the front port
M_{ARP}	acoustic mass of the rear port
C_{AF}	acoustic compliance of the front chamber
C_{AR}	acoustic compliance of the rear chamber
C_{AB}	acoustic compliance of the enclosure into which the LAT is mounted
r_A	acoustic radiation responsiveness
M_A	acoustic radiation mass

For free air operation, the enclosure compliance C_{AB} would be replaced with the appropriate acoustic impedance pairing of r_A and M_A [7].

The acoustic mass of the air in the leak M_{AL} is assumed to be negligible, due to the nature of the pass-through clearances, but the sub-circuit diagram shows where this element would be placed if needed.

It should also be pointed out that the acoustic model shown here neglects any acoustic losses that might be associated with chamber damping, port damping, and turbulent air flow. This is in line with common linear small signal modeling practice. Of course, more advanced and detailed models can be derived through modification and extension of the model shown here.

3.4. Complete Model

The complete equivalent circuit model using the electrical, mechanical and acoustic mobility analogies is shown in Figure 9 below. A circuit analysis program, such as P-SPICE [8], could be used to evaluate this model so as to predict acoustic, electric, and mechanical performance and behavior, much the same as a standard model for a conventional electrodynamic transducer. Alternatively, this model can be studied mathematically using software such as MatLab [9]. In this study, MatLab was used to conduct much of the analysis, and P-PSICE was used to cross-check the results and relationships.

Transforming the acoustic impedance into the mechanical domain, the total mechanical impedance is

$$Z_M = Z_{MD} + Z_A S_D^2 \tag{8}$$

The diaphragm velocity is

$$u_D = \frac{Bl \cdot V_G}{Z_{E,Total}} \cdot \frac{1}{Z_M} \tag{9}$$

The diaphragm volume velocity is

$$U_D = u_D S_D \tag{10}$$

The volume velocity from the leak will tend to counter the volume velocity of the diaphragm. Given that the leak acts as a shunt between the Helmholtz resonators, the volume velocity of the leak is

$$U_L = -\frac{U_D}{R_{AL}} \cdot Z_A \tag{11}$$

The total volume velocity is the sum of the diaphragm and leak volume velocities,

$$U_{Total} = U_D + U_L \tag{12}$$

Now, looking only at the front wave, the volume velocity from the port only is

$$U_{FP} = U_{Total} \cdot \frac{\frac{1}{s \cdot C_{AF}}}{\frac{1}{s \cdot C_{AF}} + s \cdot M_{AFP}} \tag{13}$$

The sound pressure level can easily be calculated from this relationship for the volume velocity of the port [5].

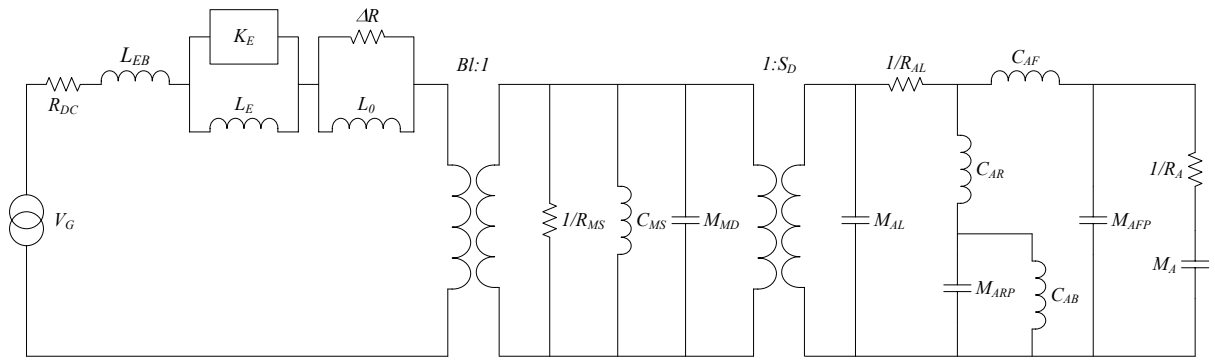

Fig. 9 Complete low frequency electro- mechano- acoustical equivalent circuit model for the LAT.

Figure 10 is useful for conceptualizing the magnitude and phase relationships of a LAT at low frequencies in a sealed box. For a conventional loudspeaker in a leak-free enclosure, the sound pressure is in phase with the acceleration of the diaphragm. The situation is identical for a leak-free LAT, but when a leak is introduced, the sound pressure begins to lead the diaphragm acceleration and the sound pressure begins to drop off. In the limit of a very large leak, the volume velocity of the leak equals the volume velocity of the diaphragm and no sound is produced.

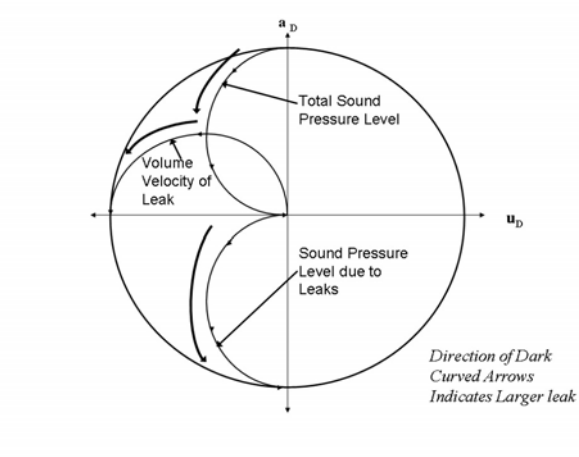

Fig. 10. Nyquist diagram of LAT complex impedance.

3.5. Model Predictions

Using this model, a LAT was simulated in MATLAB [7] with the following parameters:

M_{MD} = 400 g
C_{MS} = 0.1 mm/N
R_{MS} = 10 kg/s
S_D = 820 cm^2
l_{FP} = 8.3 cm
l_{RP} = 8.3 cm
S_{FP} = 240 cm^2
S_{RP} = 240 cm^2
$R_{AL} = \infty$
V_{AF} = 1.85 liters
V_{AR} = 1.85 liters
Bl = 18.88 T·m
R_{DC} = 2.5
L_{EB} = 0.2 mH
L_E = 50 mH
K_E = 0.280 semi-Henry
L_0 = 9 mH
ΔR = 0.2

Where l_{FP} , S_{FP} and l_{RP} , S_{RP} are the effective lengths and surface areas, and V_{AF} and V_{AR} are the equivalent compliance volumes, of the front and rear ports, respectively.

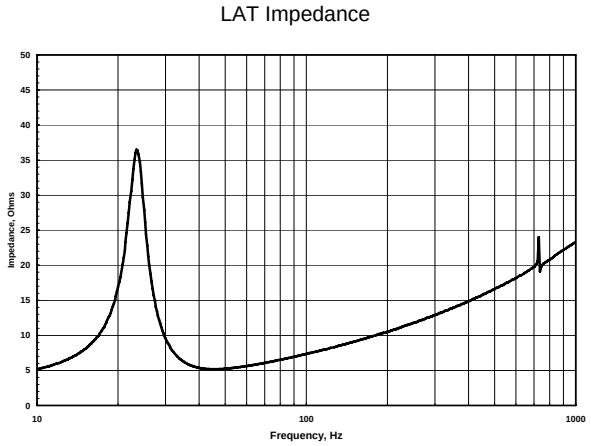

Fig. 11. Calculated electrical impedance of a LAT.

An interesting feature of the impedance curve shown in Figure 11 is the 'blip' just above 700 Hz. It was hypothesized that this feature is due to the Helmholtz resonance formed between the compliance of the air in the front and rear chambers and the mass of the air in the ports.

The resonance frequency of a Helmholtz resonator [4] is given by

$$f = \frac{c}{2\pi}\sqrt{\frac{S_P}{V_{AF} l_{FP}}} \qquad (14)$$

Here l_{FP} is the effective length of the front port, and c is the velocity of sound in air. Using the numbers above, the Helmholtz frequency is 685 Hz. This is close to the frequency of the observed 'blip' in the impedance curve. A portion of the calculated motional impedance is shown in Figure 12. The impedance has been converted to 20 $\log_{10}|Z|$ for convenience.

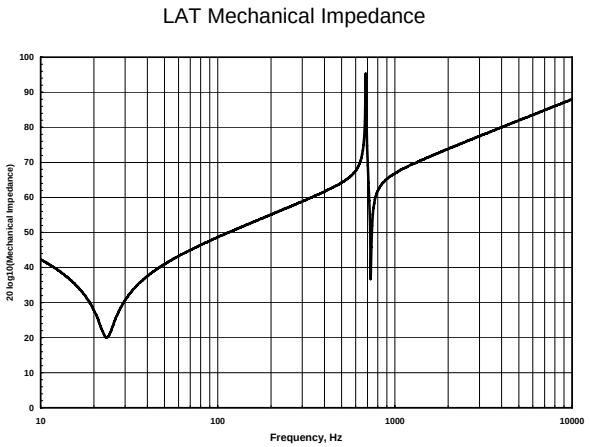

Fig. 12. Calculated mechanical impedance of a LAT in free air.

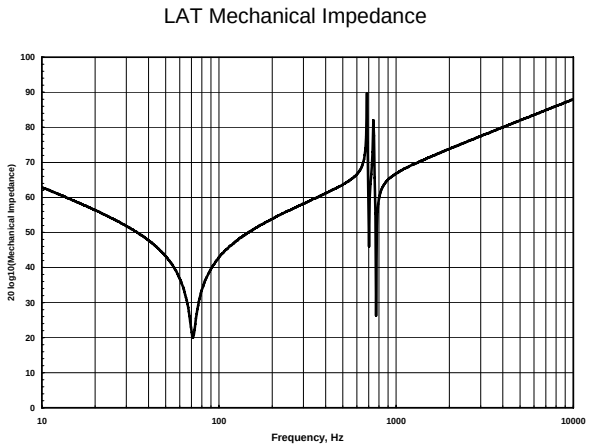

Fig. 13. Calculated mechanical impedance of a LAT mounted in a 10 liter sealed enclosure.

As shown in Figure 12, the peak in the mechanical impedance corresponds with the Helmholtz resonance, as it should. The peak in the electrical impedance is due to the dip in the mechanical impedance just after the Helmholtz resonance corresponding to a peak in the mechanical mobility of the unit.

An obvious question to ask is what happens to the mechanical impedance when the LAT is mounted in a sealed enclosure. One might expect to see two peaks, each associated with a different Helmholtz resonance. The first Helmholtz resonance would be expected to be at the same frequency as when the LAT is operated in free air and the second associated with the resonance of the air in the rear chamber trapped between the compliance of the trapped air in the LAT and the air in the enclosure.

Figure 13 shows the calculated mechanical impedance of the same LAT mounted in a 10 liter sealed enclosure. As expected, the two peaks are seen in the mechanical impedance. Likewise, there is an increase in the primary resonance of the system compared to the LAT operating in free air.

The peak in the electrical impedance just above 700 Hz shown in figure 11 corresponds with the minimum in mechanical impedance shown in figure 12. The small dip in electrical impedance just after the peak is due to the phase relationship between the blocked and motional impedance.

Mass produced LATs do not exhibit anything as obvious as the effect shown in Figure 12. A major difference between the simulated LAT in Figures 12 through 14 and production LATs, is that the mass produced LATs have the previously-mentioned small air leak, whereas the modeled results neglect the air leak. Since the air leak acts as a resistive shunt connecting the two Helmholtz resonators, it is reasonable to expect that the air leak acts to damp the peaks in the mechanical impedance.

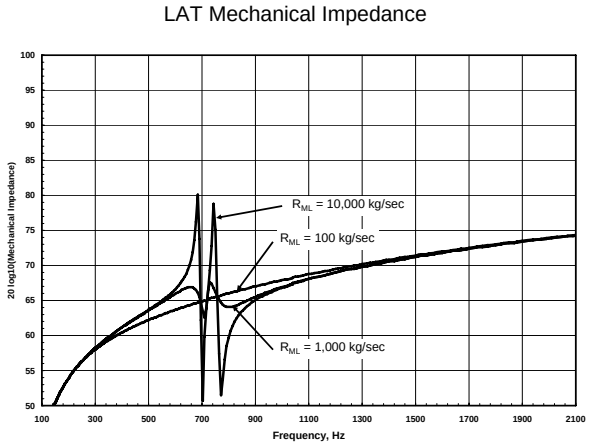

Fig. 14. Helmholtz resonances in the calculated mechanical impedance of a LAT in a 10 liter enclosure.

Figure 14 is an expanded view of Figure 13 around the Helmholtz resonance frequencies for various values of

R_{ML}, which is just R_{AL} reflected through the acoustic transformer into the mechanical domain.

From this, it can be seen that R_{ML} is highly effective in damping the Helmholtz resonance.

It is also reasonable to question what effect leakage has on the shape of the mechanical impedance at the lower frequencies. Let us again consider the LAT mounted in a sealed enclosure. One should expect that if the leak were large enough, the primary resonance frequency would decrease, approaching that of the free air resonance of the driver. This is because the leak represents a short-circuiting of the box's acoustic loading on the back side of the LAT. Figure 15 shows that this is indeed what happens.

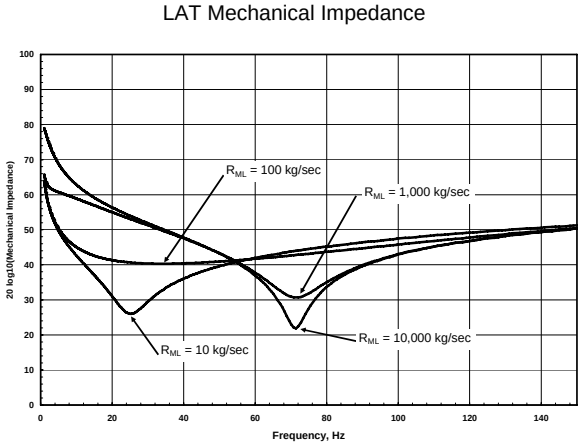

Fig. 15. Calculated mechanical impedance of a LAT at low frequencies.

With very high R_{ML}, the resonance's inflection point is sharp. This is expected, as the system resembles that of a leak-free sealed box. As the leak gets a little larger, the primary resonance is much more damped. With very large leaks, the resonance frequency shifts towards the free air resonance of the driver and is very damped. At the limit, the leak becomes so large that it offers almost no resistance at all and the LAT behaves as if it were in free air.

4. EXPERIMENTAL VERIFICATION OF THE MODEL

4.1. Electrical Impedance

Two observations were made about the electrical impedance of the LAT. The first was that at frequencies above f_{MIN}, the impedance rises at a much lower rate than the 6 dB/octave predicted by the typical loudspeaker impedance model. The second was that the measured impedance at f_{MIN} was somewhat higher than R_{DC}. It should be re-emphasized that these behaviours are common in most electrodynamic loudspeakers and are not exclusive to the LAT.

Figure 16 shows the excellent agreement between the measured and calculated electrical impedance of a six diaphragm LAT having an effective diaphragm area of 820 cm^2. The only significant deviation between the measured and calculated values of the electrical impedance is the bump around 400 Hz. The impedance increases from 16.6 Ω at 5 kHz to 23.3 Ω at 10 kHz – a rise of almost exactly 3 dB over one octave.

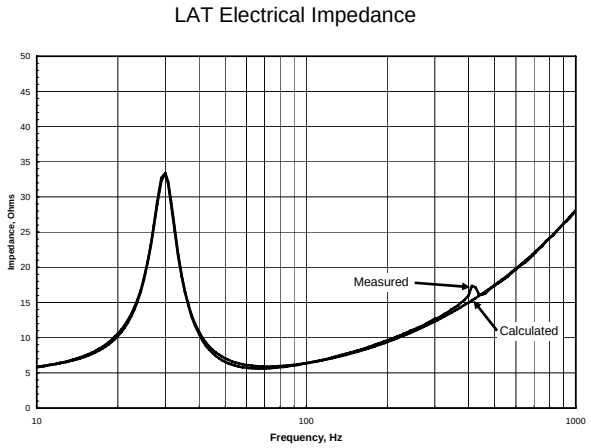

Fig. 16. Measured electrical impedance of an actual LAT and electrical impedance calculated using the LAT model.

4.2. Increase in Effective Air Mass

Section 2 makes note of the significant difference between the moving mass of the LAT as measured in free air versus the moving mass of the LAT measured in a vacuum. Figure 6 provides a helpful clue as to where this extra air mass might come from. The front and rear orifices are assumed to work as ports. Thus the

effective mechanical mass inside the ports on the front side is increased by a factor of $\left(\frac{S_D}{S_{FP}}\right)^2$, where S_{FP} is the total radiating area of the ports on front side; the rear ports would be multiplied by the same factor. This is the standard factor associated with bringing this acoustic mass through the acoustic transformer in Figure 9. This is the additional term you would add to M_{MD} in the standard calculation of M_{MS}, in addition to the contribution from the radiation impedance, as was expected from an inspection of Figure 9.

A computerized testing system was used to measure the small signal parameters of a LAT, both in vacuum and free air. The system applies a LMS fit to impedance data to derive most of the parameters. But because delta mass and delta compliance measurements are impractical with the LAT, the acceleration of one of the diaphragms (measured with an accelerometer) was used to gather the additional data to derive M_{MS}. The measured values for M_{MS} in vacuum and in free air for this particular LAT were 408g and 474g, respectively.

A very quick calculation can be made of the anticipated air mass load in the LAT. The total 'port' area per side of the LAT described above is 240 cm^2, which is equivalent to a circular port with a diameter of 17.5 cm. The physical length of the port in the LAT is quite small, so the length of the port was taken to be the same as the port end correction. The diaphragm area per side is 820 cm^2. Applying a port end correction [4] of 1.7 and assuming an air density of $\rho_0 = 1.18$ kg/m^3, we can calculate the air mass loading on the front side of the LAT as:

$$M_{FP} = S_{FP} L_{FP} \rho_0 \left(\frac{S_D}{S_{FP}}\right)^2 = 49.1g \qquad (15)$$

The actual measured air mass load was 33 grams per side suggesting an effective port end correction of 1.14. Because the predicted Helmholtz resonance of the LAT is fairly high in frequency, the air mass and mechanical mass are well coupled. Therefore, this additional air load will affect the LAT throughout the low frequency region and will affect the M_{MS} calculation of the small signal parameters.

The same calculation was made with a LAT with an effective diaphragm area of 525 cm^2 and a port area of 168 cm^2 per side. Using a port end correction of 1.14, we can calculate the air mass loading on each side of the LAT as 16.1g; the measured value was found to be 13g.

4.3. Helmholtz Resonance

Finding evidence of the Helmholtz resonators in the LAT proved difficult because the small leaks between the rods and the through holes in the diaphragms damp the resonance very effectively. In order to measure the Helmholtz resonance, an experimental LAT was fabricated that effectively sealed these leaks. An accelerometer was affixed to one of the diaphragms and the output was measured. This test was conducted both in a vacuum (where no Helmholtz effect could be active) and in free air. The free air result is shown in Figure 17 where the Helmholtz frequency appears to be centered just below 700 Hz.

For this particular LAT, S_{FP} = 240 cm^2, l_{FP} = 9.98 cm (with a port end correction of 1.14), and V_{AF} = 2.4 liters, leading to a calculated Helmholtz frequency of 550 Hz. This is reasonable agreement, given the difficulty in physically identifying some of the terms in Eq. 14 for the LAT.

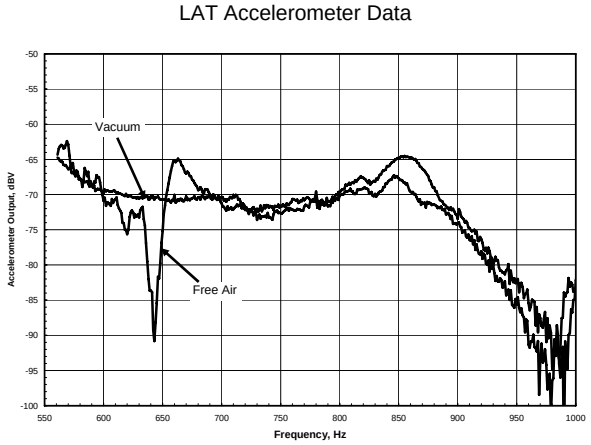

Fig. 17. Accelerometer data showing the action of the Helmholtz resonator in free air.

Another experimental LAT was fabricated with much more definable port areas and volumes. For this LAT, S_{FP} = 61.2 cm^2, l_{FP} = 5.0 cm (with a port end correction of 1.14), and V_{AF} = 1.3 liters, leading to a calculated Helmholtz frequency of 531 Hz. This agrees closely with the measured Helmholtz frequency of 500 Hz. Accelerometer data for this LAT is shown in Fig. 18.

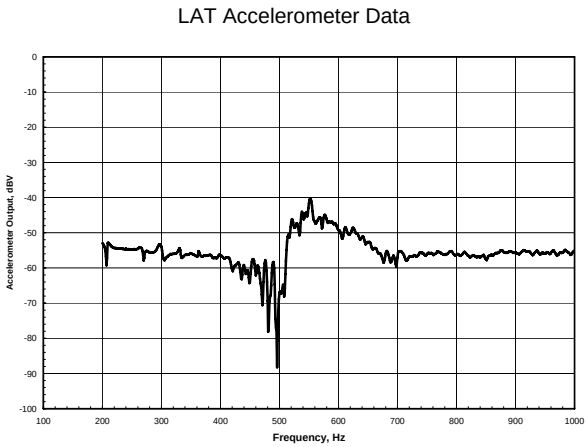

Fig. 18. Accelerometer data showing the action of the Helmholtz resonator in free air.

4.4. Frequency Response

Figures 19 and 20 show the near-field measured and calculated frequency responses for LATs with effective diaphragm areas of 820 cm^2 and 525 cm^2, respectively.

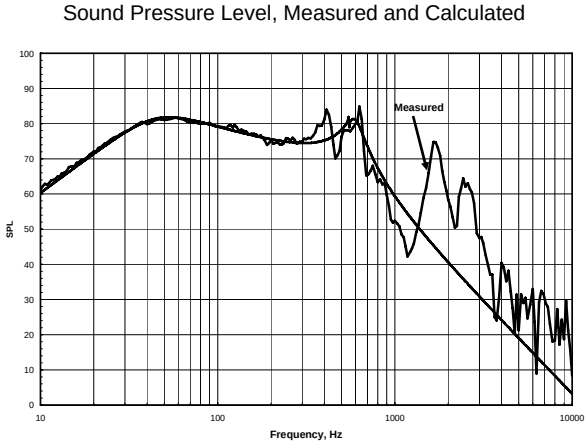

Fig. 19. Measured and calculated magnitude response for a LAT with $S_D = 820cm^2$.

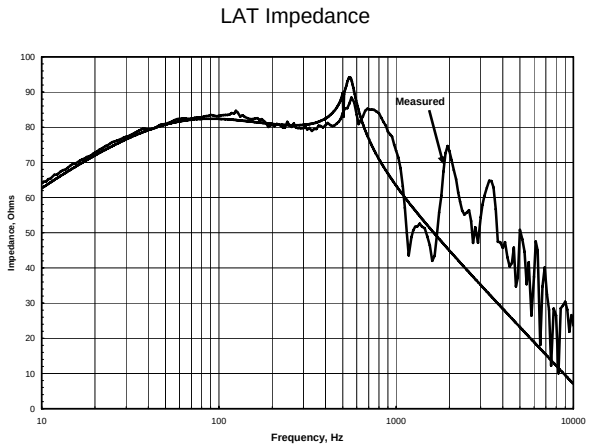

Fig. 20. Measured and calculated magnitude response for a LAT with $S_D = 525cm^2$.

Figures 19 and 20 indicated that for low frequencies, the LAT model does a good job of predicting the frequency response.

4.5. Air Leakage

The acoustic resistance of a narrow slit is given by

$$R_A = \frac{12\eta l}{t^3 w} \qquad (16)$$

where the viscosity coefficient $\eta = 1.86 \cdot 10^{-5}$ N·s/m^2 , l is the length, t is the thickness, and w is the width of the slit, [4].

Using our 820 cm^2 as an example, the acoustic resistance was calculated to be 1.78 x 10^6 N·s/m^5 per pass through. Since there are twelve pass through holes, the total acoustic resistance is 1.49 x 10^5 N·s/m^5. Multiplying this by S_D^2 gives us a value of 1000 kg/sec for R_{ML}. The electrical and mechanical parameters of a LAT were measured using an LMS fit to accelerometer and impedance data. The effects of the air load were eliminated by measuring the LAT under vacuum. The measured parameters are shown in Table 3.

Parameter	Value	Unit
R_{DC}	2.17	Ω
L_{EB}	0.137	mH
K_E	0.257	semi-H
L_0	4.97	mH
ΔR	0.268	Ω
Bl	16.62	T·m
R_{MS}	17.10	kg/s
M_{MS}	408	g
C_{MS}	0.0563	mm/N

Table 3. Small signal parameters measured in a vacuum for the LAT with $S_D = 820cm^2$.

As in section 4.3, S_{FP} = 240 cm^2, l_{FP} = 9.98 cm (with port end correction of 1.14), and V_{AF} is 2.4 liters. Recalling Figure 15, the mechanical impedance around resonance in a sealed enclosure (and thus the electrical impedance around the same frequency), is sensitive to the value of R_{ML}, taken here to be 1000 kg/sec. Figure 21 shows the measured and simulated impedance of this LAT in a 27 liter sealed enclosure. As shown in the figure, there is excellent agreement between the model and the measurement.

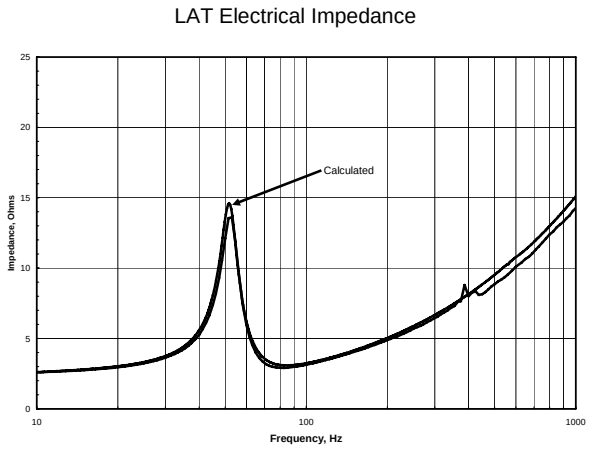

Fig. 21. Measured and calculated electrical impedance of a LAT in a small sealed enclosure.

5. DISCUSSION

Not counting the extended blocked impedance model, eight new parameters were added to the standard loudspeaker model in order to create the extended LAT model – the compliances of the front and rear chambers, the surface areas of the front and rear ports, the effective lengths of the front and rear ports, and the leakage mass and resistance terms. The first six of these terms operate to create a Helmholtz resonator and increase the air mass load on the LAT. For subwoofer applications, the Helmholtz resonant frequency lies well above the intended bandwidth. Since this resonance is well damped by the leakage resistance, with careful thought, the Helmholtz resonator could be ignored in a simplified model without loss of accuracy at low frequencies. In this case, the additional mass load can be included in the M_{MS} of the driver, leaving only one parameter not found in conventional transducers, R_{AL}. The need for this parameter is specifically related to the design and operation of this device as a LAT, as opposed to a conventional direct-radiator transducer.

Several modern enclosure modeling programs [10, 11] provide for a leakage term typically specified as Q_L, a term which was originally defined to describe the effects of a leak in a ported enclosure system [12]. It is anticipated that, with some judicious caution, this Q_L term could be used to model the effects of R_{AL} in many enclosure systems.

Thus, in spite of its seeming complexity, the LAT can easily be modeled in an enclosure using commercially available modeling software.

6. CONCLUSION

An extended small signal parameter model of the LAT was introduced that was found to be highly predictive of actual LAT behavior at low frequencies. While the model included eight parameters that are unique to the LAT, for many applications only one new parameter is important, the acoustic leakage resistance R_{AL}.

In addition, an extended blocked impedance model was introduced. While this model proved to be highly predictive of the LAT's electrical impedance, it is thought that this model is applicable to most, if not all, electrodynamic loudspeakers.

7. ACKNOWLEDGEMENTS

This work was supported by Tymphany Corporation. The authors would like to thank Mr. Knud Thorborg for communicating to us about the blocked electrical impedance model he developed that was used in this paper. In addition, the authors wish to thank Ken Kantor for his suggestions regarding the vacuum chamber measurements; Peter Andrews, David Prince, and Bob True for their valuable technical and editorial assistance; and Van Vuong for assistance with drawings and building test enclosures.

8. REFERENCES

[1] A. Unruh, R. True, *"Loudspeaker Transducers With An Alternative Form Factor",* presented at the Audio Engineering Society 117th Convention – San Francisco, CA (2004 October 5-8).

[2] A. Unruh, C. J. Struck, *"Linear Array Transducer Technology",* presented at the Audio Engineering Society 121st Convention – San Francisco, CA (2006 October 5-8).

[3] J. Vanderkooy, *"A Model of Loudspeaker Driver Impedance Incorporating Eddy Currents in the Pole Structure"* J. Audio Eng. Soc., Vol. 37, No. 3, (1989 March)

[4] C. J. Struck and S. F. Temme, *"Simulated Free Field Measurements"*, J. Audio Eng. Soc., Vol. 42, No. 6, 1994 June.

[5] L. L. Beranek, *"Acoustics"*, McGraw-Hill, 1954 (Revised Edition – Acoustical Society of America, 1993)

[6] Knud Thorborg, Tymphany internal technical communication.

[7] R. H. Small, *"Direct Radiator Loudspeaker System Analysis"*, J. Audio Eng. Soc., Vol. 20, No. 6 (1972 June).

[8] *"Application Notes Manual"*, P-SPICE version 6.0, MicroSim Corporation, 1994.

[9] W. J. Palm III, "Introduction to MatLab 7 for Engineers", McGraw-Hill, 2005.

[10] Harris Technologies, "Bass Box Pro".

[11] K. Ougaard, "UniBox".

[12] R. H. Small, "Vented-Box Loudspeaker Systems Part I: Small-Signal Analysis", J. Audio Eng. Soc., Vol. 21, No. 5 (1973 May).